Bulletin of the Seismological Society of America, 91, 6, pp. 1526–1536, December 2001

Comparison of Site Response Characteristics Inferred from Microtremors and Earthquake Shear Waves

by Masanori Horike, Boming Zhao, and Hiroshi Kawase

Abstract We investigated the validity of seismic site response characteristics estimated from microtremors by comparing them with those of earthquake motions. For this purpose we observed microtremors as well as earthquake motions using large (5-km diameter) and small (0.5-km diameter) arrays deployed on soft sediments. Specifically, we examined four estimates from microtremors: relative site amplification factors to incident shear waves, site amplification factors by the Nakamura method, resonance frequency in horizontal-to-vertical spectral ratios, and horizontal-to-vertical spectral ratios. As a result of the comparisons, we obtained the following conclusions. The relative amplification factors can be inferred from horizontal-component ratios of microtremors to a reference site within a small area of several hundred meters. The horizontal-to-vertical spectral ratios inferred by the Nakamura method partly reflect site amplification factors, but do not agree with site amplification factors. A sharp-peak frequency in the horizontal-to-vertical spectral ratios is possibly the resonance frequency. The horizontal-to-vertical spectral ratios of microtremors either agree with those of earthquake motions at some array sites or are slightly smaller at the other sites.

Introduction

Since the pioneer work by Kanai and Tanaka (1954), microtremors have been studied as a tool to estimate seismic site responses because microtremor measurements are much easier than earthquake observations and are suitable for inference of spatial variability of seismic site responses (i.e., microzonation). A main subject in the early stage was to estimate the resonant frequency (Kanai *et al.*, 1954; Katz, 1976; Ohta *et al.*, 1978; Field *et al.*, 1990). However, there are two different conclusions about the relationship of microtremor predominant frequency with local site conditions: (1) the microtremor predominant frequency is controlled by geological site conditions, (Kanai and Tanaka, 1961; Kubotera and Otsuka, 1970), and (2) it is primarily controlled by the microtremor source and propagation path (Udiwadia and Trifunac, 1973). These inconsistent conclusions suggest that the effects on microtremors of geological site conditions, microtremor source, and propagation path vary with observation sites. Therefore, the effects of the microtremor source and path must be removed to obtain reliable estimates of seismic site response characteristics.

There are two estimates of seismic site responses from which the effects of the microtremor source and path are to be removed. The first is from horizontal-component spectral ratios relative to a reference site (hereafter referred to as HH ratios) (e.g., Seo and Samano, 1993). The second is from the spectral ratios of horizontal components relative to the vertical components (hereafter referred to as HV ratios) at a site (Nakamura, 1988). Although these estimates are free from microtremor source and path effects, problems still remain in their use. Next we describe them briefly.

There are two problems for microtremor HH ratios. The first is whether they coincide with the relative site amplification factors to seismic shear-wave incidence. The second is a problem regarding areas over which the microtremor HH ratios should be used. Because microtremors are generated by human activities, especially in urban and suburban regions, the intensity of microtremor source seems to significantly vary from place to place. However, the validity of microtremor HH ratios is based on an assumption that the intensity of microtremor source (or incoming microtremors) is the same between sites. Thus, the second problem is over how large an area incoming microtremors are the same.

Nakamura (1988) proposed a method of inferring site amplification factors to incident seismic shear waves using microtremor HV ratios at a single site. This method is easily applied and directly estimates the site amplification factors without a reference site, and much research has been done to investigate the validity by observation and in theory. Summarizing the results of the research, some say that the microtremor HV ratios coincide with amplification factors of near-surface structures to incident shear waves (Lermo and Chavez-Garcia, 1993; Chavez-Garcia *et al.*, 1996; Seekins

et al., 1996; Konno and Ohmachi, 1998; Wakamatsu and Yasui, 1996), while others say they do not coincide (Field and Jacob, 1995; Lachet *et al.*, 1996).

There is another conclusion about the microtremor HV ratios. Although the microtremor HV ratios do not agree with the site amplification factor, the predominant frequency of microtremor HV ratios agrees with the resonance frequency of incident shear waves by numerical simulations (Lachet and Bard, 1994) and observations (Field and Jacob, 1995; Lachet *et al.*, 1996).

Additionally, we will compare the HV ratios between microtremors and earthquake motions for the following reason. In conventional antiseismic design, only the horizontal components are usually considered as earthquake motions input to structures. However, structures exhibit very complicated behavior when vertical seismic forces are included, and we think that it is important to consider the multicomponent earthquake input motions (Akiyama and Yamada, 1992). The stochastic simulation method (Boore, 1983; Beresnev and Atkinson, 1997) is a useful tool to synthesize strong ground motions. However, this method generates only the single horizontal component. If microtremor HV ratios coincide with earthquake HV ratios, a simple extension of the stochastic simulation method to synthesize multicomponent earthquake input motions may be feasible using microtremor HV ratios.

The first step for solving the problems described previously is to directly compare the seismic site response characteristics inferred from microtremors with those of earthquake motions under different geological conditions and different microtremor source conditions. For this comparison seismic site response characteristics of earthquake motions have to also be free from the source and path effect. This is realized by using earthquake-motion data obtained with a small array, compared with the hypocentral distance and the fault size, because the effect of the source and path on earthquake motions is almost the same at all sites, and only the local site conditions are different.

The aim of this article is to experimentally clarify which estimates from microtremor analyses are reliable seismic site responses. From the previous consideration, we make comparisons of four estimates inferred from microtremors with those from earthquake motions. Specifically, the first is made for HH ratios, and the second is for Nakamura's method. The third comparison is made between the peak frequencies of the microtremor HV ratios and the earthquake shear-wave spectra. A final comparison is made of HV ratios between microtremors and earthquake motions.

Array Observations and Data

The observations were made at Kushiro City in Hokkaido, Japan. Kushiro was selected because large spatial variations in earthquake damage were reported in the 1993 offshore Kushiro earthquake damage survey. Also, Kushiro is in a region where earthquakes occur frequently, and plenty of seismic recordings can be obtained in a short time.

The geology of Kushiro is divided by the Old Kushiro River (Fig. 1). The northern side consists of alluvial plain typified by the Kushiro Marsh, and the plateau on the southern side is the Kushiro Terrace. Figure 2 is a geological cross section below the dot-and-dash line AA′ in Figure 1. This is based on geological researches by Fujie (1995) and Ishii *et al.* (1982). The Kushiro Terrace and the alluvial plain are rather different in height above sea level and geology. The Kushiro Terrace is about 30 m higher than the plain. There is a deposit of volcanic ash (the Kushiro Group) near the surface, underlain by hard Paleocene strata (Urahoro Group). The surface topography of Kushiro Terrace includes a meteorological observatory of the Japan Meteorological Agency (JMA) on the top, a 30-m cliff to the north, a steep slope on the east, and gentle slopes to the south and west.

By contrast to the Kushiro Terrace, the plain consists of peat bog on the inland side and sand dunes on the coastal part. The distribution of thickness of the alluvial deposits is rather complicated, being thinnest near the Old Kushiro River, where it is about 10 m, and becoming deeper to the northwest, where it exceeds 70 m near the New Kushiro River (Ishii *et al.*, 1982).

We developed two arrays of different sizes to observe earthquakes and microtremors. A primary purpose for the two arrays is to investigate the spatial extent over which incoming microtremors are the same.

The smaller array (hereafter termed the JSKA array) consists of eight observation sites denoted by the solid black circles in Figure 1 within the 500-m diameter circle surrounding the Kushiro meteorological observatory (see Fig. 3). A three-component velocity seismograph was installed at each observation site. Seismic observations were carried out from 2 to 29 August 1994. Microtremor observations were made late at night on 30 August.

The larger array (hereafter termed the CIKA array) consists of the seven observation sites denoted by the solid black squares shown in Figure 1. Five of these observation sites are on the plain, and the other two observation sites are located on the Kushiro Terrace. These observation sites are part of a collaborative observation network of strong ground motions in Kushiro, implemented by the Japanese working group on the effects of surface geology on seismic motions (ESG) from September 1993. Earthquake recordings obtained by this network are already available to the public, and the earthquake-motion data obtained during the period 5 September 1993 to 5 March 1994 were used in this research. Microtremor observations were made at these observation sites on 31 August 1994 by our instruments.

Analysis

For the JSKA array two different observation systems were used for observing microtremors and earthquake motions. To estimate the relative characteristics of the two sys-

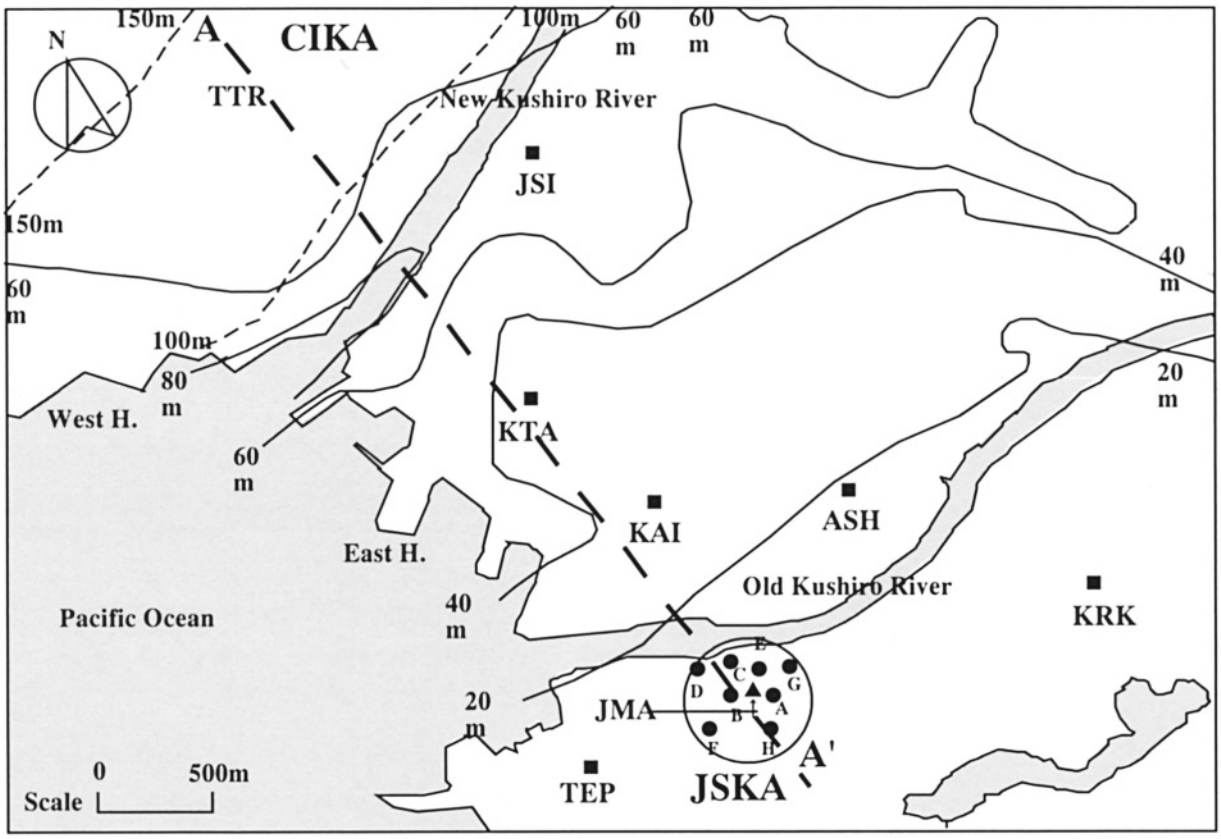

Figure 1. Contour map of the thickness of alluvial (solid line) and diluvial deposits (broken line) and the configurations of JSKA and CIKA arrays in the Kushiro district. Solid circles denote JSKA array observation sites, and solid squares denote CIKA array sites.

tems, the seismometers were huddle tested prior to the actual observations. Figure 4 shows the results of inferred relative characteristics. We see that both the horizontal and vertical relative characteristics are stable over the frequency range from 1 to 10 Hz. Therefore, subsequent microtremor and earthquake-motion analyses were directed at this frequency band, and microtremor and earthquake-motion data were compensated using the relative characteristics.

For the CIKA array the Japanese working group on ESG observed earthquake motions with a different observation system at each site. The information about the frequency response characteristics of each observation system appears in the header section of the earthquake-motion data files. We used this information to compensate earthquake-motion data.

For microtremor analysis, 10 datasets about 80 sec in length were formed from microtremor recordings when they were unaffected by noise due to traffic. Each dataset contains three components, N–S, E–W and U–D. Some examples are shown in Figure 5. Excluding the large amplitude portions at either end of the recordings, which are due to traffic near the observation site, the stationary portions enclosed in solid lines were picked out for analysis. The sampling rate is 100 samples per sec.

For the analysis of microtremors we first calculated autocorrelation functions of the three components for each dataset and then the power spectra of dataset i at array site j for the N–S component, ${}^{i}MP^{j}_{NS}$; for the E–W component, ${}^{i}MP^{j}_{EW}$; and for the U–D component, ${}^{i}MP^{j}_{UD}$, by applying an 8-sec bandwidth Bartlett lag window to the autocorrelation functions and taking their Fourier transform. The horizontal power spectra at array site j for N–S and E–W components, MP^{j}_{NS} and MP^{j}_{EW}, respectively, were the arithmetic means for 10 datasets:

$$MP^{j}_{NS}(f) = \frac{1}{10}\sum_{i=1}^{10} {}^{i}MP^{j}_{NS}(f), \tag{1}$$

$$MP^{j}_{EW}(f) = \frac{1}{10}\sum_{i=1}^{10} {}^{i}MP^{j}_{EW}(f), \tag{2}$$

where f denotes the frequency. Similarly, the vertical power spectra at array site j are

$$MP^{j}_{UD}(f) = \frac{1}{10}\sum_{i=1}^{10} {}^{i}MP^{j}_{UD}(f). \tag{3}$$

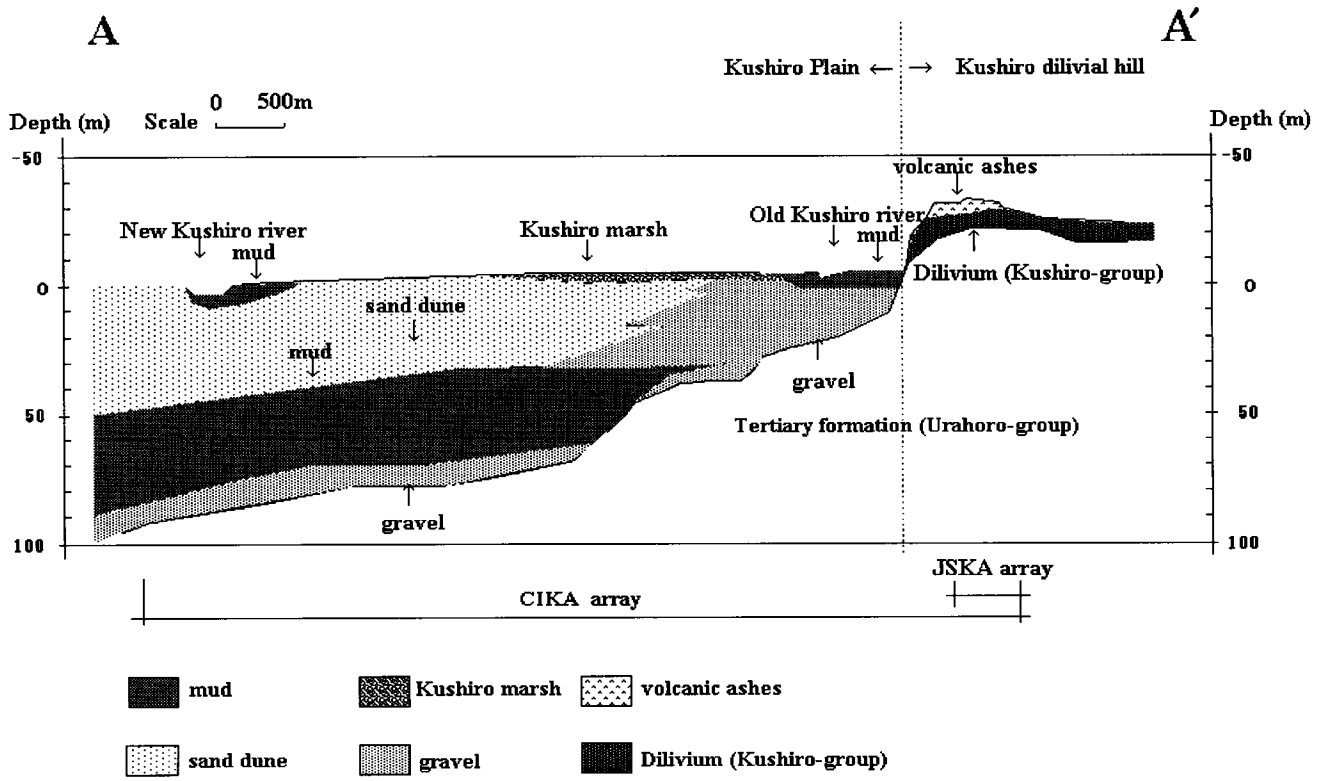

Figure 2. Geological cross section in Kushiro district below the dashed line AA′ in Figure 1.

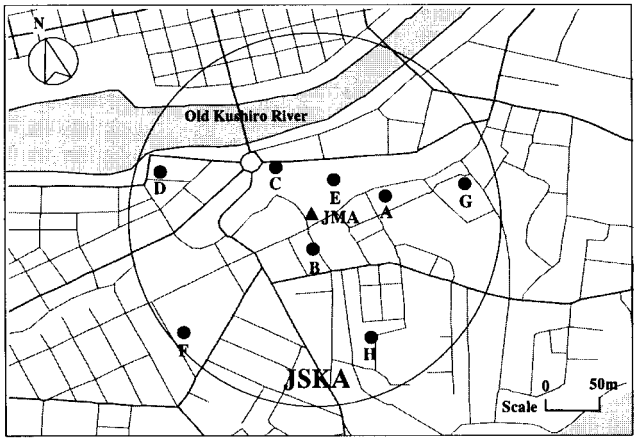

Figure 3. Configuration of JSKA array. Solid circles denote array sites, and the solid triangle denotes the location of the Kushiro JMA station.

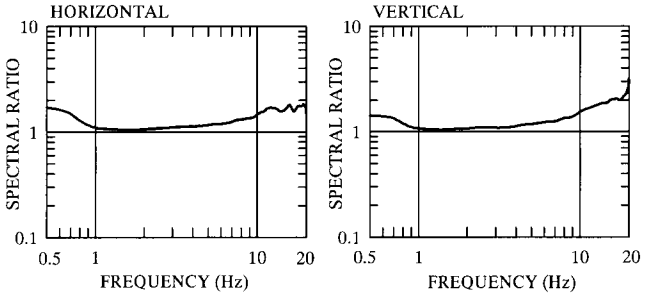

Figure 4. Relative amplitude responses of two recording systems used for this experiment. The left diagram is for the horizontal component, and the right is for the vertical component.

The horizontal power spectra of microtremors at site j, MP_H^j, are computed by the equation

$$MP_H^j(f) = MP_{NS}^i(f) + MP_{EW}^j(f). \tag{4}$$

The microtremor HH ratios at site j with respect to a reference site r are defined as

$$MHH^J(f) = \frac{\sqrt{MP_H^j(f)}}{\sqrt{MP_H^r(f)}}, \tag{5}$$

and the microtremor HV ratios at site j are

$$MHV^j(f) = \frac{\sqrt{MP_H^j(f)}}{\sqrt{MP_{UD}^j(f)}}. \tag{6}$$

For the analysis of seismic shear waves, we first determined a frequency band with an appropriate signal-to-noise (S/N) ratio. We calculated the spectral ratios of a noise por-

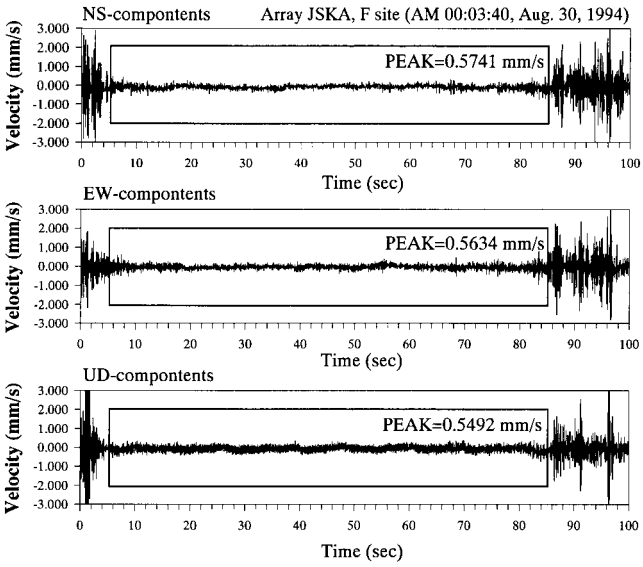

Figure 5. Example of stationary data portions with length 80 sec picked out from raw microtremor traces. Top, N–S components; Middle, E–W components; bottom, U–D components. The portions enclosed by the rectangles are used for the analyses. (Array JKSA, F site; 00:03:40, 30 August 1994).

tion of 10 sec before the *P*-wave onset to the *S*-wave portion of 10 sec. Only seismic recordings in which the ratios were at least 5 times larger in the 1 to 10 Hz frequency band were used for the analysis. Earthquake events selected in this manner are listed in Tables 1 and 2. The locations of these events are shown in Figure 6 together with the location of Kushiro.

The earthquake *S*-wave motions used for the analysis were about 25 to 40 sec long. *S*-wave spectra at site j for earthquake event i of the N–S component, ${}^iE^j_{NS}$, of the E–W component, ${}^iE^j_{EW}$, and of the U–D component, ${}^iE^j_{UD}$, were calculated by taking Fourier transforms of the autocorrelation functions for about one-tenth of the length of the *S*-wave motions. Horizontal and vertical *S*-wave spectra were defined as

$${}^iE^j_H(f) = \sqrt{{}^iE^j_{NS}(f) + {}^iE^j_{EW}(f)}, \tag{7}$$

$${}^iE^j_V(f) = \sqrt{{}^iE^j_{UD}(f)}\,. \tag{8}$$

Earthquake HH ratios at site j with respect to the reference site r and their averages for all the analyzed events are

$${}^iEHH^j(f) = \frac{{}^iE^j_H(f)}{{}^iE^r_H(f)}, \tag{9}$$

$$EHH^j(f) = \frac{1}{n}\sum_{i=1}^{n} {}^iEHH^j(f), \tag{10}$$

and earthquake HV ratios and their averages are

$${}^iEHV^j(f) = \frac{{}^iE^j_H(f)}{{}^iE^j_V(f)}, \tag{11}$$

$$EHV^j(f) = \frac{1}{n}\sum_{i=1}^{n} {}^iEHV^j(f), \tag{12}$$

where n denotes the number of earthquake events. We estimated the standard deviations for earthquake HH and HV ratios at site j:

$$\sigma^j_{HH}(f) = \left\{\frac{1}{n-1}\sum_{i=1}^{n}({}^iEHH^j(f) - EHH^j(f))^2\right\}^{1/2} \tag{13}$$

$$\sigma^j_{HV}(f) = \left\{\frac{1}{n-1}\sum_{i=1}^{n}({}^iEHV^j(f) - EHV^j(f))^2\right\}^{1/2}. \tag{14}$$

Comparison

Comparison of the HH Spectral Ratios

Figure 7 shows an example of N–S and E–W–component earthquake motions obtained with the JSKA array. Amplitude and waveforms differ from site to site. We investigated whether this variation is generated by local geological structures and whether it can be inferred using microtremor measurements.

Figure 8 shows the microtremor HH ratios (thick line) and the means plus and minus one standard deviation of the earthquake HH ratios (thin lines) for the smaller JSKA array. Observation site A was selected as the reference site because the microtremor power spectra are comparatively uniform in the frequency band.

The earthquake HH ratios are similar for analyzed earthquake events at each site (i.e., the standard deviations are small), but they differ significantly from site to site. Taking into account the small size of the array compared with the hypocentral distances (See Table 1), the effects of the earthquake source and propagation path are almost the same for all array sites. Therefore, lateral change of the local geological structure below the small array is mainly responsible for the spatial variation of the earthquake HH ratios. Consequently, the earthquake HH ratios are considered to be estimates of the relative site amplification factors of incident shear waves.

We then compare the HH ratios between earthquake motions and microtremors. We see that with the exception of observation site G where the microtremor HH ratios are somewhat bigger, the values of the microtremor HH ratios are between plus and minus one standard deviation of the earthquake HH ratios in the frequency band below 5 Hz at all observation sites. This result indicates it is possible to infer the relative site amplification factors from the microtremor HH spectral ratios.

We next examine whether microtremor HH ratios can be used to infer the relative site amplification factors in wider areas. Figure 9 shows the comparison of the HH ratios be-

Table1
Earthquake Events for Array JSKA

Event No.	Origin Time (yyyy/mm/dd) (hr:min)	Latitude (°)	Longitude (°)	M_J	Focal Depth (km)	Site							
						A	B	C	D	E	F	G	H
1	1994/08/14 10:33	44.340	150.210	6.2	47	*	*	*	*	*	*	*	–
2	1994/08/14 18:06	38.374	142.207	5.3	51	*	*	*	*	*	–	*	–
3	1994/08/16 00:13	42.000	142.280	4.6	66	*	*	*	*	*	–	*	–
4	1994/08/16 19:09	37.800	142.700	–	30	*	*	*	*	*	*	–	–
5	1994/08/18 13:42	44.440	150.500	6.3	62	*	*	*	*	*	*	*	*
6	1994/08/20 11:21	44.360	149.360	5.8	60	*	*	*	*	*	*	*	–
7	1994/08/20 13:38	44.300	149.540	6.1	65	*	*	*	*	*	*	*	*
8	1994/08/22 07:45	42.380	143.180	3.8	119	*	*	–	–	*	*	–	–
9	1994/08/23 18:04	42.570	145.160	3.9	83	*	*	*	*	*	–	*	–
10	1994/08/29 03:37	44.503	151.065	6.7	50	*	*	*	*	*	*	*	*

*Asterisks (*) and dashes (–), respectively, denote success and failure in recording.

Table 2
Earthquake Events for Array CIKA

Event No.	Origin Time (yyyy/mm/dd) (hr:min)	Latitude (°)	Longitude (°)	M_J	Focal Depth (km)	Site						
						ASH	KTA	TEP	TTR	JSI	KAI	KRK
1	1993/09/05 22:41	42.800	144.417	–	97	*	*	*	*	*	*	*
2	1993/09/11 13:55	41.950	144.717	5.5	64	–	–	–	*	*	*	*
3	1993/10/01 10:45	42.983	144.800	4.0	59	*	*	–	*	–	*	*
4	1993/10/12 00:55	32.017	138.233	7.1	388	–	–	–	–	–	*	*
5	1993/12/04 18:30	41.733	141.983	5.5	79	–	*	–	*	*	–	*
6	1994/01/26 19:03	41.683	143.950	5.6	68	–	–	–	*	*	*	*
7	1994/02/18 20:03	42.583	142.583	5.1	107	*	*	*	*	*	*	*
8	1994/03/05 17:02	42.750	143.183	4.0	101	*	*	*	*	*	*	*

*Asterisks (*) and dashes (–), respectively, denote success and failure in recordings.

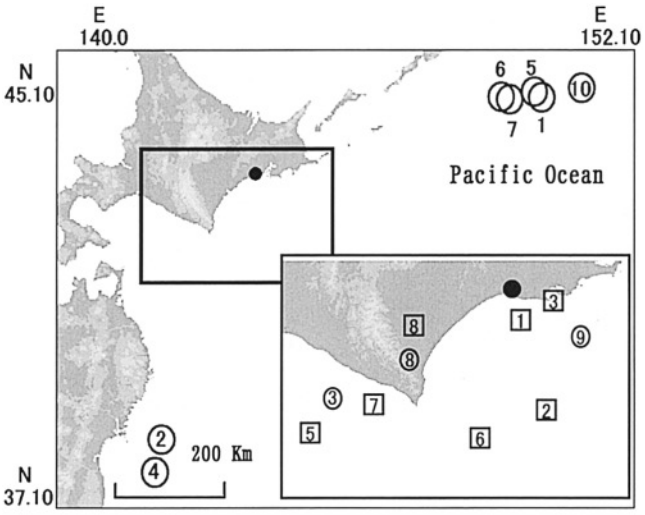

Figure 6. Location map of the earthquake events used in this study and Kushiro. The open circles denote the events for the small JSKA array, and the squares denote the events for the large CIKA array. Event no. 4 for the large array (see Table 2) is out of the map range. The circle denotes the location of Kushiro.

tween microtremors and earthquake motions for the larger CIKA array. The northwestern observation site TTR was selected as the reference station (see Fig. 3). The earthquake HH ratios exhibit the same features as those of the smaller array and are also considered to be estimates of the relative site amplification factors for the same reasons as the smaller array.

Comparing the HH ratios between earthquake motions and microtremors, although there are some observation sites such as ASH, TEP, and KRK where the peak frequencies are almost identical and the manner of their fluctuation with respect to frequency is similar, the microtremor HH ratios are outside the earthquake HH ratios by more than one standard deviation at almost all observation sites in the whole of the frequency band. Collating the results for both arrays, the incoming microtremors are the same within limited areas.

Validity of Nakamura's Method

In this section we investigate the validity of the Nakamura's method. Since the observations were made only on the ground surface of soft sediments, the site amplification factors of incident shear waves cannot be inferred directly from observed earthquake motions. Instead, we compared

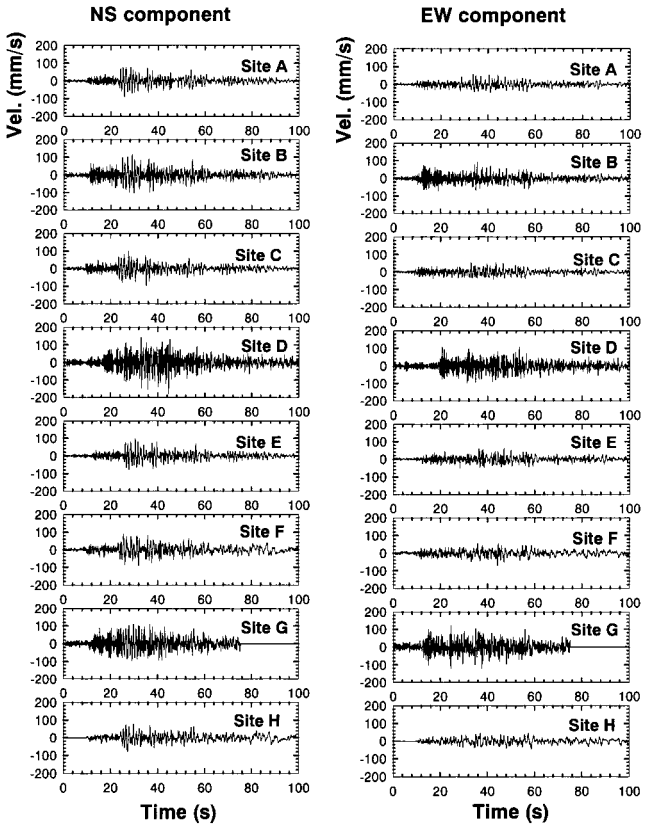

Figure 7. An example of N–S (left side) and E–W (right side) component earthquake motions radiated from earthquake event no. 8 in Table 1. They are shown from 10 sec before the *S*-wave onset.

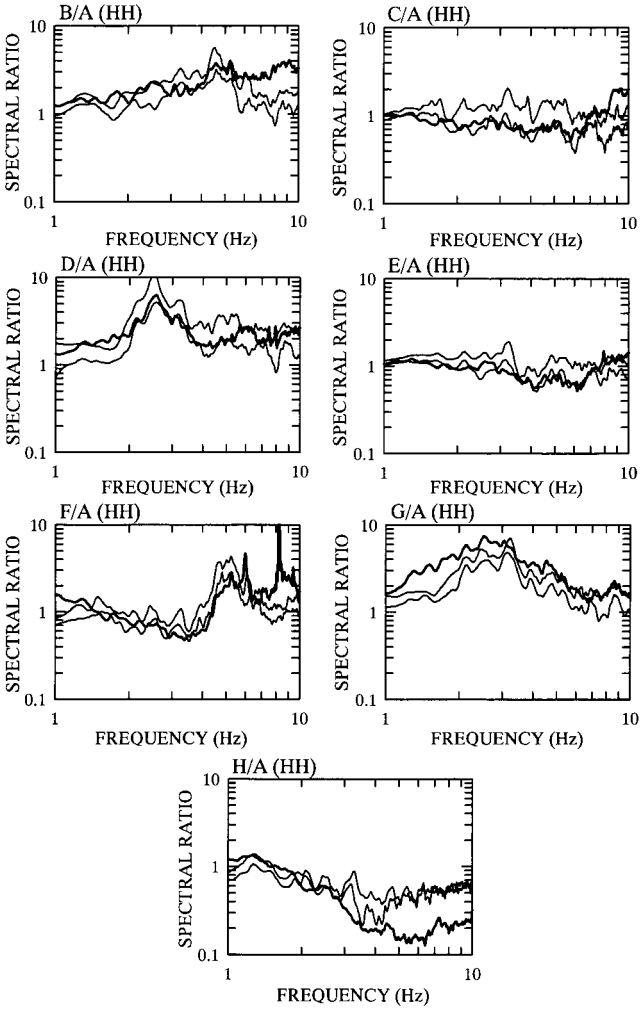

Figure 8. Comparison of the HH ratios with reference to site A between microtremors and earthquake motions for the JSKA array. Thick line is the microtremor HH ratio, and the two thin lines are the mean plus or minus one standard deviation of earthquake motions HH ratios.

the ratios of the microtremor HV ratios at the sites to those at a reference site (hereafter referred to as RHV ratios) with the earthquake HH ratios. The microtremor RHV ratio at site j to the reference site r is defined as

$$RMHV^j(f) = \frac{MHV^j(f)}{MHV^r(f)}. \tag{15}$$

If the microtremor HV ratios are in agreement with the site amplification factors, as stated by Nakamura (1988), the left-hand side of the equation should also be in agreement with the earthquake HH ratios, $EHH^j(f)$.

Figure 10 shows the comparison of the microtremor RHV ratios with the earthquake HH ratios for the smaller JSKA array. Observation site A was again selected as the reference site because vertical earthquake motions were recorded for all the events listed in Table 1. The manner of fluctuation with respect to the frequency is similar between the two ratios. However, the microtremor RHV ratios are outside the earthquake HH ratios by more than one standard deviation and are smaller than the earthquake HH ratios over the entire frequency band from 1 to 10 Hz. This result indicates that the microtremor HV ratios certainly reflect the site amplification factors in part but cannot be substituted for the site amplification factors. The same comparison for the larger CIKA array data yielded the same result as for the smaller JSKA array.

Comparison of the Peak Frequency between Microtremor HV Ratios and Earthquake Shear-Wave Spectra

Figure 11 shows the comparison of the peak frequency between microtremor HV ratio (thick lines) and seismic shear-wave spectra (thin lines) for the small JSKA array. Since the resonance frequency is generated by local site conditions, it should appear as a peak frequency common to the shear-wave spectra of all analyzed earthquake events. Examining the seismic shear-wave spectra under this condition, we find clear peaks at a frequency of 2.4 Hz for site D and at a frequency of 4.8 Hz for site F. Since the two peaks appear at different frequencies despite the close proximity

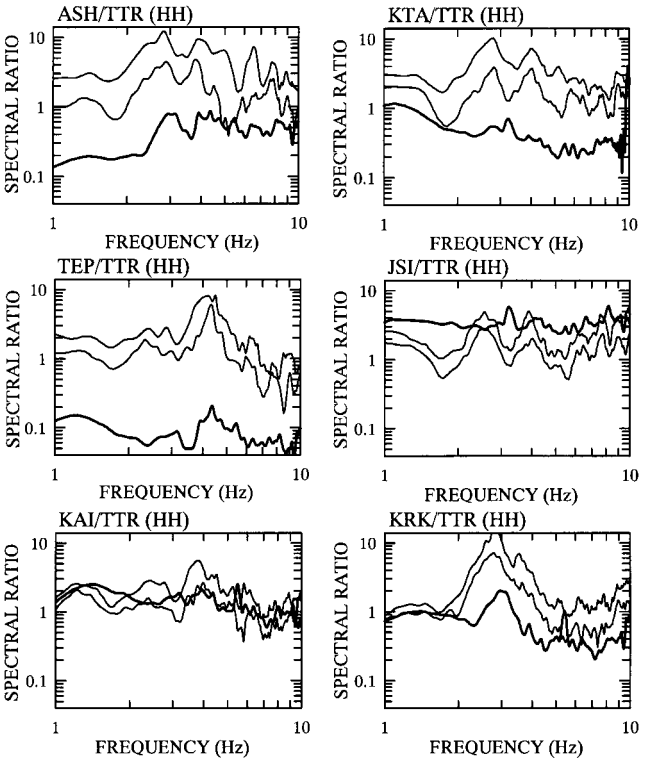

Figure 9. Comparison of the HH ratios with reference to site A between microtremors and earthquake motions for the CIKA array. The legend is the same as for Figure 8.

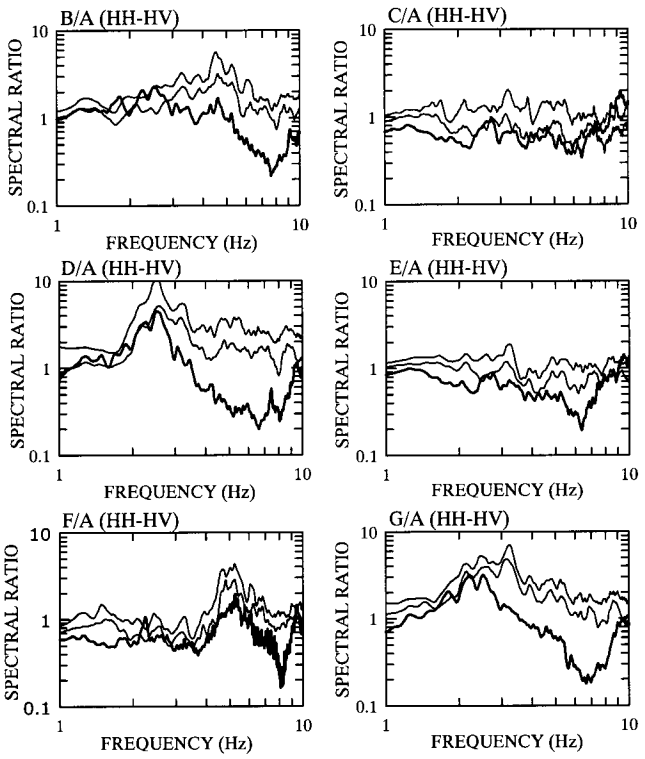

Figure 10. Comparison of the microtremor RHV ratios with the earthquake HH ratios for the small JSKA array. Thick line is the microtremor RHV ratio, and the two thin lines are the average plus or minus one standard deviation of earthquake motion HH ratio.

of the two sites, we think that these peak frequencies are generated by the effect of local site conditions.

On closer examination, we find slightly unclear but common peaks at a frequency of 3.4 Hz for site A, 4.2 Hz for site B, and 2.2 Hz for site G. Because these peaks appear at frequencies different from each other, they are possibly generated by the effects of local geological conditions.

A comparison between the peak frequencies of the microtremor HV spectra and the seismic shear-wave spectra at sites D and F shows that they are in good agreement. Furthermore, at sites A, B, and G the peak frequencies of the microtremor HV ratios are in agreement with the peak frequency of seismic shear-wave spectra, although the peak at site G is split into two. This result suggests that the microtremor HV spectrum is a reliable tool to estimate the resonance frequency.

Comparison of the HV Spectral Ratios

We compare the HV spectral ratios of earthquake motions with those of microtremors in order to investigate the feasibility of synthesis of vertical-component shear-wave motions from horizontal-component shear-wave motions using microtremor HV ratios. Figure 12 shows microtremor and earthquake HV ratios obtained from the JSKA array data. Comparing the fluctuation manner with respect to the frequency between the two ratios, they are very similar at all the array sites. Comparing the values, at observation sites A, B, and G, the microtremor HV spectral ratios are in good agreement with the earthquake HV ratios over almost the whole of the frequency band. Meanwhile, at observation sites C, D, E, and F, the microtremor ratios are close to the earthquake ratios but are a little smaller.

The same comparison for the larger CIKA array data yielded results similar to the smaller JSKA array data. Collating the results of comparing HV ratios for the two arrays, if microtremor HV ratios are used instead of earthquake HV ratios, the vertical-component earthquake motions are sometimes overestimated.

Discussion

We showed that the microtremor HH ratios for the large array are not in agreement with the earthquake HH ratios. This may be explained as follows. There are two primary sources of microtremors. One is human activity such as traffic and factories and the other is natural sources such as wind and waves. The weather was so fine during microtremor observations that human activities were primary sources of microtremors observed in Kushiro. Human activity level certainly altered from site to site within the large array because

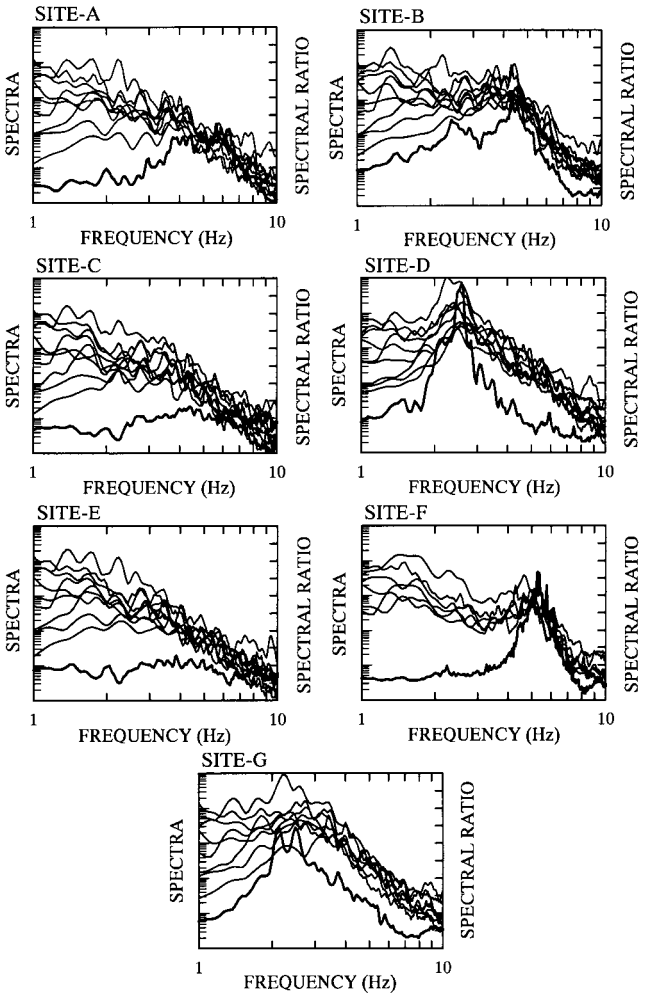

Figure 11. Comparison between the peak frequency of earthquake shear-wave spectra and microtremor HV ratios for the JSKA array. Thick line is the microtremor HV ratio, and the thin lines are earthquake shear-wave spectra for the events listed in Table 1.

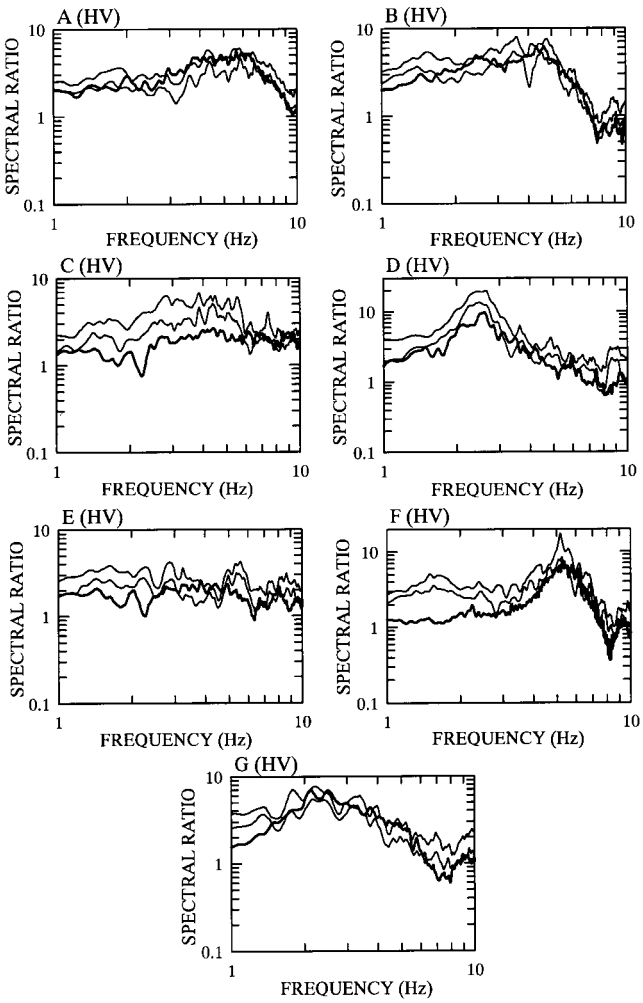

Figure 12. Comparison of the HV ratios between microtremors and earthquake motions for the CIKA array. Thick line is the microtremor HV ratio, and the two thin lines are the mean plus or minus one standard deviation of the earthquake-motion HV ratio.

the area was composed of various zones such as port, business, residence, and farm. Therefore, we think that the intensity of incoming microtremors (or density of microtremor sources) varied within the extent of the larger array. This may be the reason why the microtremor HH ratios did not agree with the earthquake HH ratios for the large array.

The previous discussion raises a problem of how wide the area is over which incoming microtremors are the same. However, this is practically impossible to solve. For practical use of the microtremor HH ratios, areas should be limited to an extent of a few hundred meters in diameter.

We indicated that the microtremor HV ratio is a good tool to infer the resonant frequency. Let us consider the reason for this. A key point for this consideration is to understand what types of elastic waves are primarily contained in microtremores especially on soft sediments like Kushiro. Thus, we discuss it first.

As described previously, microtremors are primarily generated by human activities as well as natural sources. Since these microtremor sources are on ground surface, surface waves are excited most efficiently (See equations 7.145 and 7.146 by Aki and Richards [1980]). In addition, since the geometrical spreading factor of the surface waves is smaller than that of body waves, the attenuation of the surface waves is also smaller than that of the body waves. Therefore, surface waves are considered to be dominantly contained in microtremors, especially for sites on soft sediments. This has been confirmed experimentally by Horike (1985), Milana *et al.* (1996), and Liu *et al.* (2000). Also, the array experiments conducted at five points in Kushiro by Miyakoshi *et al.* (1997) showed that microtremors were composed of surface waves. Therefore, it is reasonable to think that microtremors analyzed in this study also primarily contained surface waves.

The agreement of the peak frequency between the mi-

crotremor HV ratios and the earthquake shear-wave spectra can be explained as follows. The peak frequency in the HV spectral ratios of Rayleigh waves becomes clear at sites having layer interface of high impedance ratios in near surface geological structures (Nogoshi and Igarashi, 1971) because of the minima of the vertical-component spectra of the Rayleigh waves at the peak frequency. Furthermore, Tokimatsu (1997) showed that as the impedance ratio increases, the peak frequency in the HV spectral ratios of Rayleigh waves approaches the resonant frequency to *S*-wave incidence. Consequently, as described previously, since vertical-component microtremors are mainly composed of Rayleigh waves, the peak frequency of the microtremor HV ratios agrees with the peak frequency of the earthquake shear-wave spectra at sites having layer interfaces with high impedance ratios in near-surface geological structures. This is the reason why the sharp peak frequency of the earthquake spectra is in agreement with the sharp peak frequency of microtremor HV ratios at sites D and F, as shown in Figure 11.

When the microtremor HV ratios are used to infer the resonance frequency of sites, we face a problem of how large the microtremor HV ratio at peak frequency needs to be in order to be regarded as a reliable estimate. This is very difficult to answer precisely. However, our experience has taught us that the peak frequency at which the microtremor HH ratio is at least 4 to 5 is likely to be a reliable estimate.

We explained that the agreement between the peak frequencies of earthquake spectra and microtremor HV spectra is based on microtremors being composed of surface waves. However, this introduces another difficulty in accounting for the agreement between the HH ratios of microtremors and earthquake motions, because we analyzed the shear-wave portion for estimating earthquake HH ratios. However, a promising result was shown by Satoh *et al.* (1998). They indicated that the *S*-wave portion except for its early part is primarily composed of surface waves generated by near-site inhomogeneities. If this is also true in Kushiro, the agreement of the HH ratios between microtremors and earthquake motions can be understood reasonably. Moreover, it may also account for the result that the HV ratios of microtremors exhibit the same manner in fluctuation as those of earthquake motions, and that the values are either the same or the microtremors are a little smaller.

Conclusion

In this study, we investigated the validity of seismic site response characteristics inferred from microtremors. For this purpose we made direct comparisons between microtremors and earthquake motions observed with two arrays of different size deployed over soft sediments in Kushiro City, Hokkaido, Japan. As a result, we have obtained the following results: (1) The microtremor HH ratios are in agreement with the earthquake HH ratios for the small array but are not for the large array; (2) the microtremor RHV ratios are not in agreement with the earthquake HH ratios, though they are similar in their manner of fluctuation with respect to the frequency; (3) Sharp peaks in the microtremor HV ratios are in agreement with the predominant frequency of the sites; and (4) Microtremor HV ratios are either in agreement with the earthquake HV ratios at some sites or a little smaller than at the other sites.

These results indicate that two estimates from microtremors can be used to infer seismic site response characteristics: one is the microtremor HH ratio for estimating the relative site amplification factors and the other is the peak frequency for estimating the resonance frequency. However, these should not be used unconditionally. The HH ratios should be used within limited areas (a diameter of several hundred meters), while the peak frequency in the HV ratios should be chosen as the resonance frequency only when the value of the peak is large (at least 4 to 5). The second result indicates that microtremor HV ratios cannot be substituted for site amplification factors quantitatively, though they reflect the site amplification factors in part. The fourth result suggests that if the microtremor HV ratios are used to synthesize the vertical earthquake motions, they are sometimes overestimated slightly.

Acknowledgments

The ESG Committee provided some earthquake-motion data obtained from the Kushiro strong seismic observation network. We gratefully acknowledge this assistance. We also express our appreciation to Eiji Kitamura and Kazuhiro Shibata, graduate students, Department of Architecture, Osaka Institute of Technology and Shin'ichi Matsushima of Shimizu Corporation, for their kind cooperation with the observations. Comments from anonymous review were invaluable in improving the manuscript.

References

Aki, K., and P. G. Richards (1980). *Quantitative Seismology*, W. H. Freeman and Co., San Francisco, California, Vol. **1,** 315.

Akiyama, H., and S. Yamada (1992). Response of multi-story frames subjected to combined horizontal and vertical ground motions, *J. Struct. Constr. Eng.* **437,** 51–57 (in Japanese with English abstract).

Beresnev, I. A., and G. M. Atkinson (1997). Modeling finite-fault radiation from the ω^n spectrum, *Bull. Seism. Soc. Am.* **87,** 67–84.

Boore, D. M. (1983). Stochastic simulation of high-frequency ground motions based on seismological models of the radiated spectra, *Bull. Seism. Soc. Am.* **73,** 1865–1894.

Chavez-Garcia, F. J., L. R. Sanchez, and D. Hatzfeld (1996). Topographic site effects and HVSR. A comparison between observation and theory, *Bull. Seism. Soc. Am.* **86,** 1559–1573.

Field, E. H., and K. H. Jacob (1995). A comparison and test of various site-response estimation techniques, including three that are not reference site dependent, *Bull. Seism. Soc. Am.* **85,** 1127–1143.

Field, E. H., S. E. Hough, and K. H. Jacob (1990). Using microtremors to assess potential earthquake site response: a case study in Flushing Meadows, New York City, *Bull. Seism. Soc. Am.* **80,** 1456–1480.

Fujie, T. (1995). *Geological map of Kushiro*, Fukada Geological Institute, Kushiro (in Japanese), scale 1:50,000.

Horike, M. (1985). Inversion of phase velocity of long-period microtremors to the *S*-wave-velocity structure down to the basement in urbanized areas, *J. Phys. Earth* **33,** 59–96.

Ishii, K., H. Kagawa, M. Takashima, and T. Ishida (1982). *Soil Deposits*

of Kushiro City, Kushiro Branch of Hokkaido Registered Architect Association, Kushiro (in Japanese).

Kanai, K., and T. Tanaka (1961). On microtremors. VIII, *Bull. Earthquake Res. Inst.* **39,** 97–114.

Kanai, K., and T. Tanaka (1954). Measurement of the microtremor, *Bull. Earthquake Res. Inst.* **32,** 199–209.

Katz, L. J. (1976). Microtremor analysis of local geological conditions, *Bull. Seism. Soc. Am.* **66,** 45–60.

Konno, K., and T. Ohmachi (1998). Ground-motion characteristics estimated from spectral ratio between horizontal and vertical components of microtremor, *Bull. Seism. Soc. Am.* **88,** 228–241.

Kubotera, A., and M. Otsuka (1970). Nature of nonvolcanic microtremor observed on the Aso-Caldera, *J. Phys. Earth.* **18,** 115–124.

Lachet, C., and P. Y. Bard (1994). Numerical and theoretical investigations on the possibilities and limitations of the 'Nakamura' technique, *J. Phys. Earth.* **42,** 377–397.

Lachet, C., D. Hatzfeld, P.-Y. Bard, N. Theodulidis, C. Papaioannou, and A. Savvaidis (1996). Site effects and microzonation in the city of Thessaloniki (Greece) Comparison of different approaches, *Bull. Seism. Soc. Am.* **86,** 1692–1703.

Lermo, J., and F. J. Chavez-Garcia (1993). Site effects evaluation using spectral ratios with only one station, *Bull. Seism. Soc. Am.* **83,** 1574–1594.

Liu, H.-P., D. M. Boore, W. B. Joyner, D. H. Oppenheimer, R. E. Warrick, W. Zhang, J. C. Hamilton, and L. T. Brown (2000). Comparison of phase velocities from array measurements of Rayleigh wave associated with microtremor and results from borehole shear-wave velocity profile, *Bull. Seism. Soc. Am.* **90,** 666–678.

Meremonte, M., A. Frankel, E. Cranswick, D. Carver, and D. Worley (1996). Urban seismology: Northridge aftershocks recorded by multiscale arrays of portable digital seismographs, *Bull. Seism. Soc. Am.* **86,** 1350–1363.

Milana G., S. Barba, E. Del Pezzo, and E. Zambonelli (1966). Site response from ambient noise measurements: new perspective from an array study in Central Italy, *Bull. Seism. Soc. Am.* **86,** 320–328.

Miyakoshi, K., H. Okada, T. Sasatani, T. Moriya, S. Ling, S. Saito, K. Ishikawa, H. Nagumo, N. Sakajiri, and T. Koyanagi (1997). Estimation of geological structure in Kushiro City using microtremor, *in Report of Test Study B Under Contract with the Ministry of Education*, 80–87 (in Japanese).

Nakamura, Y. (1988). Inference of seismic responses of surficial layer based on microtremor measurement, Quarterly Report on Railroad Research, Vol. 4, Railway Technical Research Institute, 18–27 (in Japanese).

Nogoshi, M., and T. Igarashi (1971). On the amplitude characteristics of microtremor (part 2), *Zisin (J. Seism. Soc. Japan)* **2,** no. 24, 26–40 (in Japanese with English abstract).

Ohta, Y., H. Kagami, N. Goto, and K. Kudo (1978). Observation of 1 to 5 second microtremors and their application to earthquake engineering. I. Comparison with long-period acceleration at the Tokachi-Oki Earthquake of 1968, *Bull. Seism. Soc. Am.* **68,** 767–779.

Satoh, T., H. Kawase, and S. Matsushima (1998). Difference of empirical site characteristics obtained from microtremors, S-wave, P-wave, and their theoretical interpretation, *Zisin* (*J. Seims. Soc. Jpn.*) **51,** 291–318 (in Japanese with English abstract).

Seekins, L. C., L. Wennerberg, L. Margheriti, and H.-P. Liu (1996). Site amplification at five locations in San Francisco, California: a comparison of S-waves, codas, and microtremor, *Bull. Seism. Soc. Am.* **86,** 627–635.

Seo, K., and T. Samano (1993). Use of microtremors for prediction of seismic motion, in Report of General Research (A) under Contract with the Ministry of Education, 198–200 (in Japanese).

Tokimatsu, K. (1997). Geotechnical site characterization using surface waves, in *Earthquake Geotechnical Engineering,* Ishihara (Editor), A. A. Balkema, Rotterdam, The Netherlands, 1333–1368.

Udwadia, F. E., and M. D. Trifunac (1973). Comparison earthquake and microtremor ground motion in El Centro, *Bull. Seism. Soc. Am.* **63,** 1227–1253.

Wakamatsu, K., and Y. Yasui (1996). Possibility of estimation for amplification characteristics of soil deposits based on ratio of horizontal to vertical spectra of microtremors, in *Proc. 11th World Conference on Earthquake Engineering,* Paper No. 1526.

Architecture Department
Osaka Institute of Technology
5-16-1, Omiya, Asahi-ku
Osaka 535-8585, Japan
(M.H.)

Geo-Research Institute
4-3-2, Itachibori, Nishi-ku
Osaka, 550-0012, Japan
(B.Z.)

Graduate School of Human-Environment Studies
Kyusyu University
6-10-1, Hakozaki, Higashi-ku
Fukuoka 812-8581, Japan
(H.K.)

Manuscript received 31 May 2000.